

A NIR Fluorescent Probe Benzopyrylium Perchlorate-based for Visual Sensing and Imaging of SO₂ Derivatives in Living Cells

Xiao Ye Luo

Zunyi Medical and Pharmaceutical College

Juan Xie

Zunyi Medical and Pharmaceutical College

Guang Lian Zhao

Zunyi Normal University

Gui Yong Li

Zunyi Medical and Pharmaceutical College

Hang Da Qu

Zunyi Medical and Pharmaceutical College

Yu Zhu Yang (✉ yangyuzhus@163.com)

Zunyi Medical and Pharmaceutical College

Research Article

Keywords: Benzopyrylium perchlorate, Near infrared, Fluorescent probe, Sulfur dioxide derivatives, Cells imaging

Posted Date: September 8th, 2022

DOI: <https://doi.org/10.21203/rs.3.rs-2015777/v1>

License: © ⓘ This work is licensed under a Creative Commons Attribution 4.0 International License.

[Read Full License](#)

Abstract

Endogenous sulfur dioxide (SO₂), as a gas signal molecule, has a certain physiological functions. Understanding the role of endogenous SO₂ in human physiology and pathology is of great significance to the biological characteristics of SO₂, which bring

challenges to develop fluorescent probes with excellent performance. Herein, we rationally designed and constructed a novel near-infrared bioprobe benzaldehyde-benzopyrylium (BBp) by employing the nucleophilic addition benzopyrylium perchlorate fluorophore and benzaldehyde moiety by means of C=C/C=O group that serves as both fluorescence reporting unit. Probe BBp exhibit excellent sensing performance with fluorescent "On-Off" rapid response (100 s) and long-wavelength emission (670 nm). With the treatment of HSO₃⁻, the color of BBp solution obviously varies from purple to colorless, and the fluorescent color varies from red to colorless. By the fluorescence and colorimetric changes, probe BBp was capable of sensitive determination HSO₃⁻ with low limits of detection (LOD) of 0.43 μM, realizing visual quantitative monitoring SO₂ derivative levels. Due to the low phototoxicity and good biocompatibility, it was successfully applied to monitor SO₂ derivatives and fluorescence imaging in HepG2 and HeLa living cells. Hopefully, this work supplies a new strategy for designing NIR fluorescent probes for quantitative determination SO₂ derivatives in biological samples.

Introduction

Endogenous sulfur dioxide (SO₂) is discovered as an important endogenous gasotransmitter after hydrogen sulfide (H₂S), carbon monoxide (CO), and nitric oxide (NO) [1, 2]. Endogenous SO₂ can be produced endogenous reactivating species (RSS) by the metabolism of sulfur, a class of sulfur-containing compounds that play a crucial role in redox homeostasis, cellular signaling, and metabolic regulation [3–6]. Under physiological conditions, SO₂ is readily hydrated and transformed to its derivatives sulfite (SO₃²⁻) and bisulfite (HSO₃⁻) [7–9]. SO₂ in the body can be inhaled not only through the respiratory tract, but also through diet and medication. Increasing evidences demonstrated that endogenous SO₂ and its derivatives (HSO₃⁻ / SO₃²⁻) take part in some physiological processes such as vasorelaxant, antioxidative effects, and regulating cardiovascular structure and function [10–13]. In a manner of speaking, the SO₂ biological function can be replaced to HSO₃⁻ / SO₃²⁻. It is noteworthy that abnormal changes in endogenous SO₂ levels are associated with a series of physiological diseases, such as lung injury, cancer, respiratory, abnormal glucose metabolism, and other diseases [14–18]. Considering the contradictory nature of endogenous SO₂, we deem that it is necessary to deeply explore the intracellular role of SO₂ derivatives, to provide valuable information for pathological mechanism of cell cellular regulatory, which prompted us to focus on developing analytical tools for effectively monitor SO₂ derivatives in living cells.

Compared with traditional analytic technique, fluorescence assay is one of attractive bioanalytical tool. Fluorescent probe technology has been proved more practical due to its many outstanding properties

such as non-invasive, high temporal resolution, high sensitivity as well as real-time detectability, which are widely used in biochemical analysis, environmental analysis, biological imaging, medical diagnosis and other fields[19–23]. Recently, with regard to SO₂ derivatives determination and recognition, a variety of functional and practical fluorescent probes with highly selective and sensitive have been built and these probes have achieved satisfactory results in sensing and fluorescence imaging in living cells and in vivo, whose different recognition mechanism mainly including intramolecular charge transfer (ICT) effect, Michael addition, resonance energy transfer (FRET), and nucleophilic addition with aldehyde groups [24–28]. Among these probes, their excitation and emission wavelengths are mainly take advantage of the UV-Visible region (Table S1), only a few probes displayed large Stokes shifts and rapid responses [29–31], which are essential for sensitive detection SO₂ derivatives in living cells. Near-infrared (NIR) fluorescent probes can effectively avoid the interference of spontaneous fluorescence, self-absorption as well as low phototoxicity in biological systems, which is beneficial to improve the biological imaging efficiency[32–36]. Needless to say, there is still ample sufficient space to exploit a novel near-infrared fluorescent probe for sensing SO₂ derivative with tailored property.

Benzopyrylium salt is an ideal fluorescent skeleton with large shift and long wavelength emission[37, 38]. Based on this, we selected benzopyrylium perchlorate as fluorophore, benzaldehyde unit as SO₂ derivative recognition unit, and reasonably designed and fabricated a new near infrared biological probe benzaldehyde-benzopyrylium (BBp), to achieve sensitive and rapid detection of SO₂ derivative levels. The sensing mechanism as presented in Scheme 1, based on irreversible nucleophilic addition of HSO₃⁻ toward -C = O and -C = C-, with HSO₃⁻ treatment, it reacts with the probe BBp of the aldehyde group and the furan ring double bond, the emission intensity at 670 nm was gradually decreased and the response time reach the maximum within 100 s, building a near-infrared fluorescence "On-Off" sensitive and quick response SO₂ derivative sensing platform. More importantly, the NIR probe BBp presented low optical toxicity and good cell permeability, the probe BBp had been successfully applied for sensing of SO₂ derivatives and fluorescent imaging in HepG2 and HeLa living cells.

Experimental Section

Synthesis of probe BBp

Benzopyrylium perchlorate was fabricated according to the method of reference [37]. The mixture of benzopyrylium perchlorate (356 mg, 1 mmol) and p-benzaldehyde (134 mg, 1.2 mmol) were added into a 50 mL two-bottle, and dissolved in 10 mL acetic acid. The mixture was stirred and reflow for 12 h, and the reaction process was monitored by TLC. After the reaction, the black solid compound as probe BBp (0.216 g, yield: 44%) was obtained by filtration and purification of dichloromethane/ethanol (V/V, 100/1) by chromatography column. ¹HNMR (600 MHz, DMSO-d₆) δ 10.11 (s, 1H), 8.62 (s, 1H), 8.13 (s, 1H), 7.99 (d, J = 9.0 Hz, 1H), 7.93 (d, J = 7.8 Hz, 1H), 7.78 (m, 2H), 7.52 (d, J = 7.8 Hz, 1H), 7.49 (s, 1H), 7.35 (s, 1H), 3.75 (s, 4H), 2.93 (d, 4H), 1.89–1.86 (m, 2H), 1.26 (s, 6H). ¹³CNMR (DMSO-d₆) δ 193.15, 172.40, 161.73,

159.62, 157.13, 149.57, 141.95, 137.15, 134.45, 133.13, 131.68, 131.25, 130.51, 125.53, 121.26, 120.72, 96.31, 47.34, 27.36, 27.35, 21.78, 21.43. HRMS (ESI-MS, m/z): calcd for C₂₅H₂₆NO₂⁺: 372.1958; found: 372.1958 [M].

Sample preparation process

The analysis of solution preparation process: Na₂HPO₄, NaH₂PO₄, KCl and NaCl were used as raw materials, and phosphate buffer solution (PBS, 0.01 M, pH 7.4) was prepared according to the standard method. The analytical solution of probe BBp was prepared in DMF solution (100.0 μM). The test solution 0.01 M of NaHSO₃, amino acids, anionic and cationic salts was prepared with ultrapure water. All the experimental water is ultra-pure water.

Feasibility experiment analysis process: take 10 μL probe BBp analysis solution and different amounts of test solution NaHSO₃ (0 – 100 μM) into a 1.5 mL centrifuge tube, then dilute the solution to 1000 μL with PBS buffer solution (0.01 M, pH 7.4), and incubate for 3 min. Finally, the absorption spectrum data were collected. Under the same experimental conditions, the selectivity experiment is carried out: 10 μL probe BBp solution was mixed with 50 μM amino acids, biological ion and other substances, and diluted to 1000 μL with PBS buffer solution (0.01 M, pH 7.4). After incubation for 3 min, fluorescence spectra were determined under excitation wavelength of 530 nm. All analytical experiments were carried out at room temperature.

Cells viability determination and fluorescence imaging

The cells viability was determined by CCK8 method. Firstly, 8000 of HeLa cells and HepG2 cells were cultured in 96-well plates at 5% CO₂ and 37 °C for 24 h. Different amounts of probe BBp (0–30 μM) were added and incubated for 24 h. Whereafter, adding 10 μL CCK8 dealt with each well and continued incubation for 2 h, and then the cells were washed with PBS solution several times. Finally, absorbance was collected by ThermoFisher, Japan. Its relative cell viability (%) was calculated by the following formula:

$$\text{Cell vitality} = (\text{OD}_{\text{treated}} / \text{OD}_{\text{control}}) \times 100\% - 1$$

Among them, OD_{treated} and OD_{control} represent the optical density values measured in the presence and absence of probe BBp.

The HeLa cells and HepG2 cells were cultured in glass plates for 24 h before imaging experiment. The two kinds of cells were first handled with probe BBp (10 μM) for further incubation for 10 min, and then the cells were washed with PBS solution for several times, and then with different concentrations of HSO₃⁻ (10 and 50 μM) were treated for 10 min. Finally, fluorescence images were collected by fluorescence confocal image. The emission blue channel wavelength range of the collected image data is λ_{em} = 566 – 697 nm (λ_{ex} = 561 nm).

Results And Discussion

Design and characterization of fluorescent probe BBp

The benzaldehyde-benzopyrylium (BBp) fluorescence probe was synthesized by employing the main p-phthalaldehyde and benzopyrylium perchlorate by means of the nucleophilic addition reaction as depicted in Fig.S1. Benzopyrylium perchlorate is an ideal long-wavelength emission skeleton and benzaldehyde unit as SO₂ derivative recognition unit, which ensures that the probe conjugate system exhibits near-infrared emission (670 nm). Meanwhile, aldehyde group and the furan ring double bond are an excellent recognizing sites for detection SO₂ derivatives (HSO₃⁻/SO₃²⁻) because of its high reaction performance, which could meet the requirements for the sensitive determination under the visible light excitation (530 nm). The fluorescent probe BBp was characterized by ¹H NMR, ¹³C NMR, and HRMS (Fig. S2-S4, Supplementary information).

Optical properties of HSO₃⁻ sensing by probe BBp

The sensing ability of probe BBp to HSO₃⁻ was investigated by fluorescence and colorimetric performance under optimum conditions. Firstly, the UV-Vis spectra of the probe BBp (10 μM) was estimated in PBS buffer solution (0.01 M, pH 7.4, containing 1% DMF) at room temperature. As shown in Fig. 1A, the original probe BBp solution exhibited a maximal absorption band centered at 560 nm and has another a weak absorption peak at 300 nm. In contrast, Upon treatment with HSO₃⁻ (50 μM), the main absorption peak at 560 nm was decreased significantly, while a new generated absorption band at 340 nm. It was observed that the color of the corresponding solution remarkable changed from purple to colorless under visible light (illustrated in Fig. 1A), indicating that the probe BBp could achieve the visual detection of HSO₃⁻ levels by colorimetric method. This results speculated that HSO₃⁻ could destroy the conjugate system of the probe, causing a steady decrease in the long absorption wavelength.

Furthermore, under excitation at 530 nm, the initial probe BBp showed a strong emission peak at 670 nm, and its near-infrared fluorescence emission intensity gradually weakened with the increase of HSO₃⁻ concentration (0–100 μM) and the color of fluorescence changes from red to colorless green as seen on the inset (Fig. 1B). Meanwhile, the results of spectral properties suggest that this phenomenon may be attributed to the nucleophilic addition reaction between the aldehyde group and double bonds of furan ring in the probe BBp and HSO₃⁻. The fluorescence intensity ratio (F / F_0) of probe BBp exhibited an excellent linear relationship between the HSO₃⁻ concentration (5–60 μM) with a relatively high coefficient of determination ($R^2 = 0.991$) (F represents the fluorescence intensity of probe BBp changing with different concentrations of HSO₃⁻, F_0 represents the fluorescence intensity of initial probe BBp)(Fig. 1C). The LOD is calculated according to the equation $LOD = 3\sigma / k$, where σ is the standard deviation of blank sample $N = 10$, k is the slope of the linear regression equation), the calculated detection of limit was 0.43 μM. The results confirmed that probe BBp enables a sensitive and quantitative determination of HSO₃⁻ by means of NIR fluorescence “On-Off”. The fluorescence probe BBp that we construct has a good linear

range and a relatively low LOD compared with previously reported fluorescent probes for detection HSO_3^- levels (Table S1). This long emission probe BBp is comparable and performs better than other methods. It is worth mentioning that the fairly low LOD are much lower than the level of tissues and organs in living organisms generation endogenous SO_2 levels [39, 40], illustrating that the probe BBp is feasible for the actual determination of SO_2 derivatives in vivo.

In addition, time-dependent is an important parameter in analysis and detection. The response time fluorescence intensity of the reaction between probe BBp and HSO_3^- with different concentrations (0–50 μM) was recorded. It can be seen from Fig. 1D that the reaction probe BBp with HSO_3^- proceeded resulting in the fluorescence intensity gradually decrease and remain unchanged after 100 s at room temperature. The probe BBp has a fast response to HSO_3^- in the buffer solution. The long-wavelength probe BBp could meet well the requirement for real-time monitoring of HSO_3^- levels in living cells. It follows that probe BBp has the advantages of low detection limit, high sensitivity and fast response, affirming that probe BBp has excellent sensing performance for detecting SO_2 derivatives.

Sensing mechanism study

In order to validate the mechanism by which the probes BBp sensitively sense HSO_3^- levels, we collected the evidence through HRMS analysis. According to the characteristic peak of mass spectrum, the mass charge ratio (m/z) corresponding to the main characteristic peak at 372.1958 attributed to the compound mass peaks of probe BBp [M], while the calculated value was 372.1958 (Fig. 2A). In addition, when a certain amount of HSO_3^- was added into the probe BBp, the characteristic peak at 534.1269 [M + H] emerged, it was mainly attributed to the reaction product of recognition site 1 (furan ring double bond) and recognition site 2 (aldehyde group) in probe BBp with HSO_3^- (Fig. 2B). The calculated m/z value of the reaction product was 534.1267. It can be seen that the theoretical value is consistent with the experimental value. Combined with the spectral results, we speculated that the irreversible nucleophilic addition reaction between the furan ring double bond and aldehyde group in the probe BBp and HSO_3^- was reasonable [41–44](Fig. 2C). It was further confirmed that the destruction of conjugated system by irreversible nucleophilic addition reaction was the main reason that the fluorescence of probe BBp changed from red to colorless. Taken together, HRMS spectral analysis have well supported our speculative sensing mechanism.

Anti-interference ability and pH effect

Anti-interference capability is an important factor to evaluate the effectiveness of probes in analyzing biological samples. To this end, the chemoselectivity of probe BBp for detection HSO_3^- was studied. Several exogenous substances including amino acids (100 μM of Cys, Hcy and GSH), physiological anions and cations (50 μM of Na^+ , K^+ , Ca^{2+} , Mg^{2+} , Cu^{2+} , Fe^{3+} , Cl^- , I^- , F^- , H_2PO_4^- , CO_3^{2-} , HCO_3^- , and HS^-) were selected as bio-related substances. As shown in Fig. 3A, the introduction of these potential interferes

has no effect on the fluorescence intensity of probe BBp. When $\text{HSO}_3^- / \text{SO}_3^{2-}$ were added, the fluorescence intensity of the probe BBp decreased significantly. Except for HS^- and mercaptan molecules at a higher concentration can cause mild fluorescence intensity change. This is mainly because $\text{HSO}_3^- / \text{SO}_3^{2-}$ can undergo nucleophilic addition reaction with the double bond and aldehyde group in the furan ring [26, 38, 44], but its influence on the detection of HSO_3^- by probe BBp in biological system is negligible. The presence of these high concentration of exogenous interferences has little interference, making clear that the NIR probe BBp has high selectivity and good anti-interference ability to HSO_3^- . The anti-interference experiments suggested that the probe could be used for determination SO_2 derivatives in complex biological systems.

Subsequently, the influence of pH fluctuations on the detection performance of probe BBp was evaluated. We adjusted the PBS buffer of probe BBp to different changed in the range of pH 3.5–10.5, revealing that probe BBp had excellent acid-alkali resistance (Fig. 3B). It shows that the probe realized the determination of SO_2 derivatives under physiological pH conditions. Whereafter, the photostability of probe BBp was assessed under UV light irradiation at 365 nm. The emission intensity of the synthesized probe BBp displays hardly fluctuation upon continuous irradiation for 60 min (Fig.S5), which confirmed that the synthesized probe BBp has better photostability. Based on the above research, the excellent performance of probe BBp has the ability to determine the content of SO_2 derivatives in real biological samples.

Cytotoxicity and intracellular fluorescence imaging

Based on the analysis performance evaluation results of the probe, the designed probe BBp exhibited superior recognition capability, especially including good sensitivity, excellent photostability and low phototoxicity. Consequently, the fluorescence imaging capability of the probe BBp for sensing SO_2 derivatives in living cells was estimated. HeLa cells and HepG2 cells were selected as imaging model cells. Firstly, the cytotoxicity of different doses of probe BBp toward HeLa cells and HepG2 cells were analyzed by the standard CCK8 assay. As presented in Fig. S6, the survival rate of HeLa cells and HepG2 cells reached 80% even if the high-concentration of probe BBp (30 μM) (the cell survival rate was calculated by formula $1 - 1$). The cytotoxicity experiments were confirmed that the probe BBp had relatively low toxicity and good biocompatibility for living cells. These results suggested that the probe BBp meets the requirements for the analysis and detection in biological systems.

Subsequently, the NIR probe BBp was used to monitor HSO_3^- levels and imaging in living cells. Firstly, the intake time-dependence imaging of living cells uptake probe BBp was performed. As described in Fig. 4, the probe BBp (10 μM) was incubated with HeLa cells and HepG2 cells at different periods of time. The intracellular red fluorescence obvious appeared in the red channel with increasing time, and the red fluorescence became significantly brighter to stable until 20 min after incubation (Fig. 4A-D), suggesting that the probe BBp displays an excellent cell uptake ability and intracellular stability. These results

demonstrated that 10 min is suitable for imaging incubation experiments and probe BBp has potential applications in real-time monitoring of SO_2 in living cells.

Inspired by the excellent imaging results, the effectiveness of the probe BBp for imaging the SO_2 derivatives levels in living was further carried out. As expected, when HepG2 cells and HeLa cells were incubated with 10 μM probe BBp only for 10 min, obvious red fluorescence were observed from the cells in the red channel (Fig. 5A). However, when HeLa cells and HepG2 cells were pre-treated with different concentrations of exogenous HSO_3^- (10 μM and 50 μM), and significantly became blurred fluorescence imaging is observed (Fig. 5B and 5C), indicating that the intracellular probe BBp can be efficiently quenched by exogenous HSO_3^- . The change from red fluorescence to non-fluorescent signal observed in cells further explained that the probe BBp can be an ideal tool for the effectively monitoring SO_2 in living cells.

Conclusion

In summary, a near-infrared fluorescent “On - Off” probe BBp was rationally designed to achieve sensitive detection of HSO_3^- levels in living cells. Based on the nucleophilic addition reaction mechanism, the fluorescence intensity decreased gradually at 670 nm, and the color of the corresponding solution was observed to change from red to colourless under UV lamp (356 nm), realizing visual recognition of HSO_3^- . In vitro experiments, the probe BBp with rapid response, high selectivity, and sensitivity, and the detection of limit was as low as 0.43 μM . The recognition mechanism was verified by HRMS. A fluorescence “On - Off” sensitive sensing SO_2 derivatives platform was successfully constructed. Due to the advantages of biocompatibility and good cell permeability, it was successfully used to monitor exogenous HSO_3^- and fluorescence imaging in HepG2 and HeLa cells. We believe that the rational design strategy using benzopyrylium perchlorate as a long-wave fluorophore can be exploited to construct long-wavelength fluorescent probes, which are ideal further applications for bioassay and imaging applications.

Declarations

Acknowledgements This work was financially supported by Zunyi City and School Joint Project (No. Zun City Kehe HZ Word (2019) 205).

Authors' Contributions Xiao Ye Luo performed investigation, data curation, writing - original draft and editing. Juan Xie : Investigation, data curation. Guang Lian Zhao: Conceptualization. Gui Yong Li: Investigation, Methodology. Hang Da Qu: Methodology. Yu Zhu Yang performed performed cell culture experiments and a cellular cytotoxicity test, writing–review & editing, supervision, project ad-ministration, and funding acquisition.

Funding The authors gratefully acknowledge the Zunyi City and School Joint Project (No. Zun City Kehe HZ Word (2019) 205) for the financial support.

Data Availability All data generated or analyzed during this study are included in this published article.

Code Availability Not Applicable.

Supplementary Information The online version contains supplementary material available at [https:// doi.org/ 10. 1007/ s xxxxxxx](https://doi.org/10.1007/sxxxxxx).

Conflict of Interest: The authors declare that they have no conflict of interest in the publication of this article.

Ethics approval/declarations Not applicable.

Consent to Participate Not applicable.

Consent for Publication Not applicable.

References

1. Yang QQ, Tian QQ, Ji N, Duan X H, Zhu X H, Zhang Y L, He W (2022) A novel fluorescent probe for the detection of sulfur dioxide derivatives and its application in biological imaging. *N J Chem* 46:1483-8.
2. Xu ZC, Ge YF, Chen KY, Liu MH (2022) A ratiometric water-soluble fluorescent probe for the detection of sulfur dioxide derivative in sinusitis mice model. *Talanta* 237:122972.
3. Liu FT, Li N, Chen YS, Yu HY, Miao JY, Zhao BX (2022) A quinoline-coumarin near-infrared ratiometric fluorescent probe for detection of sulfur dioxide derivatives. *Anal Chim Acta* 1211:339908.
4. Zheng DB, Zhang TR, Huang JJ, Wang M, Cao ZX, Huang Y, Yang ZQ , Deng Y, Fang YY (2022) Indole-incorporated-benzoeindolium as a novel mitochondrial and ratiometric fluorescent probe for real-time tracking of SO₂ derivatives in vivo and herb samples. *Dyes Pigments* 198:109973.
5. Zheng YL, Chai ZH, Tang W, Yan S, Dai F, Zhou B (2021) A multi-signal mitochondria-targetable fluorescent probe for simultaneously discriminating Cys/Hcy/H₂S, GSH, and SO₂ and visualizing the endogenous generation of SO₂ in living cells. *Sensors Actuat B: Chem* 330:129343.
6. Yang LL, Yang N, Gu PL, Zhang YH, Gong XY, Zhang S, Li JW, Ji LG, He GJ (2022) A novel naphthalimide-based fluorescent probe for the colorimetric and ratiometric detection of SO₂ derivatives in biological imaging. *Bioorg Chem* 123:105801.
7. Zhang Q, Hu XX, Dai XM, Sun JY, Gao F (2021) A photostable reaction-based A-A-A type two-photon fluorescent probe for rapid detection and imaging of sulfur dioxide. *J Mater Chem B* 9:3554-62.
8. Hu B, Zhu JW, Shen JJ, Yang L, Jiang CL (2022) A portable sensing platform using an upconversion-based nanosensor for visual quantitative monitoring of mesna. *Anal Chem* 94:7559-66.
9. Zeng LT, Chen TH, Chen BQ, Yuan HQ, Sheng RL, Bao GM (2020) A distinctive mitochondrion-targeting, in situ-activatable near-infrared fluorescent probe for visualizing sulfur dioxide derivatives and their fluctuations in vivo. *J Mater Chem B* 8:1914-21.

10. Zhang XY, Yan HM, Huo FJ, Chao JB, Yin CX (2021) Dual-emission NIR fluorescent probe sensitive response biological microenvironment and sulfur dioxide. *Sensors Actuat B Chem* 344:130244.
11. Li ZY, Cui XL, Yan YH, Che QL, Miao J Y, Zhao BX, Lin ZM (2021) A novel endoplasmic reticulum-targeted ratiometric fluorescent probe based on FRET for the detection of SO₂ derivatives. *Dyes Pigments* 188:109180.
12. Liu T, Zhao WJ, Guo ZL, Zhai YZ, Zhang WJ, Yang XF, Chen DD, Yin CX (2022) Water-soluble improved NIR ratiometric fluorescent probe for specific imaging sulfur dioxide in cancer cell membranes and living mice. *Sensors Actuat B Chem* 368:132098.
13. Chao JB, Wang Z, Zhang YB, Huo FJ, Yin CX (2021) A near-infrared fluorescent probe targeting mitochondria for sulfite detection and its application in food and biology. *Anal Methods* 13:3535-42.
14. Zhang WJ, Liu T, Huo FJ, Ning P, Meng XM, Yin CX (2017) Reversible ratiometric fluorescent Probe for sensing bisulfate/H₂O₂ and its application in zebrafish. *Anal Chem* 89:8079-83.
15. Ma YY, Tang YH, Zhao YP, Lin WY (2019) Rational design of a reversible fluorescent probe for sensing sulfur dioxide/formaldehyde in living cells, zebrafish, and living mice. *Anal Chem* 91:10723-30.
16. Chen G, Zhou W, Zhao CY, Liu YX, Chen T, Li YL, Tang B (2018) Rationally optimized fluorescent probe for imaging mitochondrial SO₂ in HeLa cells and zebrafish. *Anal Chem* 90:12442-8.
17. Shen WL, Hu GX, Xu HH, Sun W, Hu YH, Yang WG (2022) Construction and evaluation of ratiometric fluorescent probes based on a 7-aminocoumarin scaffold for the detection of SO₂ derivatives. *Dyes Pigments* 198:109971.
18. Lovati M R, Manzoni C, Daldossi M, Spolti S, Sirtori CR (1996) Effects of sub-chronic exposure to SO₂ on lipid and carbohydrate metabolism in rats. *Arch Toxicol* 70:164-73.
19. Gu J, Liu Y, Shen JW, Cao YY, Zhang L, Lu YD, Wang BZ, Zhu HL (2022) A three-channel fluorescent probe for selective detection of ONOO(-) and its application to cell imaging. *Talanta* 244:123401.
20. Zhang XY, Huo FJ, Zhang YB, Yue YK, Yin CX (2022) Dual-channel detection of viscosity and pH with a near-infrared fluorescent probe for cancer visualization. *Analyst* 147:2470-6.
21. Huang TH, Yan SR, Yu YB, Xue YS, Yu YY, Han CP (2022) Dual-responsive ratiometric fluorescent probe for hypochlorite and peroxyxynitrite detection and imaging in vitro and in vivo. *Anal Chem* 94:1415-24.
22. Li ZH, Cheng J, Huang P, Song WH, Nong L, Huang L, Lin WY (2022) Imaging and detection of hepatocellular carcinoma with a hepatocyte-specific fluorescent probe. *Anal Chem* 94:3386-93.
23. Cai ST, Liu C, Jiao XJ, He S, Zhao LC, Zeng XS (2020) A lysosome-targeted near-infrared fluorescent probe for imaging of acid phosphatase in living cells. *Org Biomol Chem*. 2020;18:1148-54.
24. Gao WJ, Ma YY (2020) Design of a FRET-based fluorescent probe for the reversible detection of SO₂ and formaldehyde in living cells and mice. *New J Chem* 44(32): 13654-13658.
25. Wang LL, Zhao LL, Xu ZC, Ma YY, Wang XF, Sun Q, Liu H (2021) Rapid detection of SO₂ in living cells and zebrafish by using an efficient near-infrared ratiometric fluorescent probe with large emission

- shift. *Microchem J* 160:105703.
26. Yang YZ, Qing M, Luo XY, Xie J, Zhang LN (2022) A dual-response fluorescent probe for discriminative sensing of hydrazine and bisulfite as well as intracellular imaging with different emission. *Spectrochim Acta A Mol Biomol Spectrosc.* 270:120795.
 27. Li DP, Tang FY, Wen K, Yang ZK, Xiao HB, Zhou ZY (2022) A ratiometric fluorescent probe for SO₂ derivatives based on a new coumarin-hemicyanine dye in living cells. *Microchem J* 175:107233.
 28. Yue LZ, Huang HW, Song WH, Lin WY (2022) A near-infrared endoplasmic reticulum-targeted fluorescent probe to visualize the fluctuation of SO₂ during endoplasmic reticulum stress. *Chem Eng J* 431:133468.
 29. Wang K, Wang W, Chen SY, Guo JC, Li JH, Yang YS, Wang XM, Xu Chen, Zhu HL (2021) A novel near-infrared rhodamine-derived turn-on fluorescence probe for sensing SO₃²⁻ detection and their bio-imaging in vitro and in vivo. *Dyes Pigments* 188:109229.
 30. Han SH, Zhang H, Wang JP, Yang L, Lan MH, Wang BH, Song XZ (2021) Rational development of dual-ratiometric fluorescent probes for distinguishing between H₂S and SO₂ in living organisms. *Anal Chem* 93:15209-15.
 31. Li YB, Zhu YL, Cai XZ, Guo JM, Yao CP, Pan QL, Wang XF, Wang KN (2021) A benzothiazole-based near-infrared fluorescent probe for sensing SO₂ derivatives and viscosity in HeLa cells. *Spectrochim Acta A Mol Biomol Spectrosc.* 251:119457.
 32. Wang YF, Niu HY, Wang K, Wang G, Liu JW, James TD, Zhang H (2022) mtDNA-specific ultrasensitive near-infrared fluorescent probe enables the differentiation of healthy and apoptotic cells. *Anal Chem* 94:7510-9.
 33. Ren HX, Huo FG, Wen W, Yin CX (2022) Engineering an ESIPT-based fluorescent probe for dual-channel (Vis/ NIR) ratiometric monitoring of intracellular sulfur dioxide by single wavelength excitation. *Dyes Pigments* 199:110111.
 34. Kong XY, Shuang SM, Zhang YT, Wang Y, Dong C (2022) Dicyanoisophorone-based fluorescent probe with large Stokes shift for ratiometric detection and imaging of exogenous/endogenous hypochlorite in cell and zebrafish. *Talanta* 242:123293.
 35. Chung JW, Kim HJ, Li HD, Yoon JY (2021) Reasonably constructed NIR fluorescent probes based on dicyanoisophorone skeleton for imaging ONOO⁻ in living cells. *Dyes Pigments* 195:109665.
 36. Wu CY, Ni ZQ, Li PJ, Li YQ, Pang X, Xie RH, Zhou ZL, Li HT, Zhang YY (2020) A near-infrared fluorescent probe for monitoring and imaging of β-galactosidase in living cells. *Talanta* 219:121307.
 37. Zhang GH, Quan W, Li YX, Song WH, Lin WY (2022) Near-Infrared Mitochondria-Targetable Single-Molecule probe for Dual-Response of viscosity and sulfur dioxide in vivo. *Spectrochim Acta A Mol Biomol Spectrosc.* 270:120796.
 38. Zhao YP, Ma YY, Lin WY (2019) A near-infrared and two-photon ratiometric fluorescent probe with a large Stokes shift for sulfur dioxide derivatives detection and its applications in vitro and in vivo. *Sensors Actuat B Chem* 288:519-26.

39. DU SX , Jin HF, Bu DF, Zhao X, Geng B, Tang CS, Du JH (2008) Endogenously generated sulfur dioxide and its vasorelaxant effect in rats. *Acta Pharmacol Sin* 29 (8): 923–930.
40. Meng ZQ, Li JL, Zhang QX, Bai WM, Yang ZH, Zhao Y, Wang FQ (2009) Vasodilator effect of gaseous sulfur dioxide and regulation of its level by Ach in rat vascular tissues. *Inhalation toxicology* 21:1223-8.
41. Zhong KL, Yao Y, Sun XF, Wang YT, Tang LJ, Li XP, Zhang JL, Yan XM, Li JR (2022) Mitochondria-targeted fluorescent turn-on probe for rapid detection of bisulfite/sulfite in water and food samples. *J Agric Food Chem* 70:5159-65.
42. Ren HX, Huo FG, Wu X, Liu XG, Yin CX (2021) An ES IPT-induced NIR fluorescent probe to visualize mitochondrial sulfur dioxide during oxidative stress in vivo. *Chem Commun* 57:655-8.
43. Yang YZ, Qiu WX, Xu ZY, Sun Z, Qing M, Li NB, Luo HQ (2022) Rational design of a fluorescent probe for specific sensing of hydrogen peroxide/glucose and intracellular imaging applications. *Spectrochim Acta A Mol Biomol Spectrosc.* 277:121254.
44. Cai FC, Hou B, Zhang SP, Chen H, Ji SC, Shen XC, Liang H (2019) A chromenoquinoline-based two-photon fluorescent probe for the highly specific and fast visualization of sulfur dioxide derivatives in living cells and zebrafish. *J Mater Chem B* 7:2493-8.

Scheme

Scheme 1 is available in the Supplementary Files section.

Figures

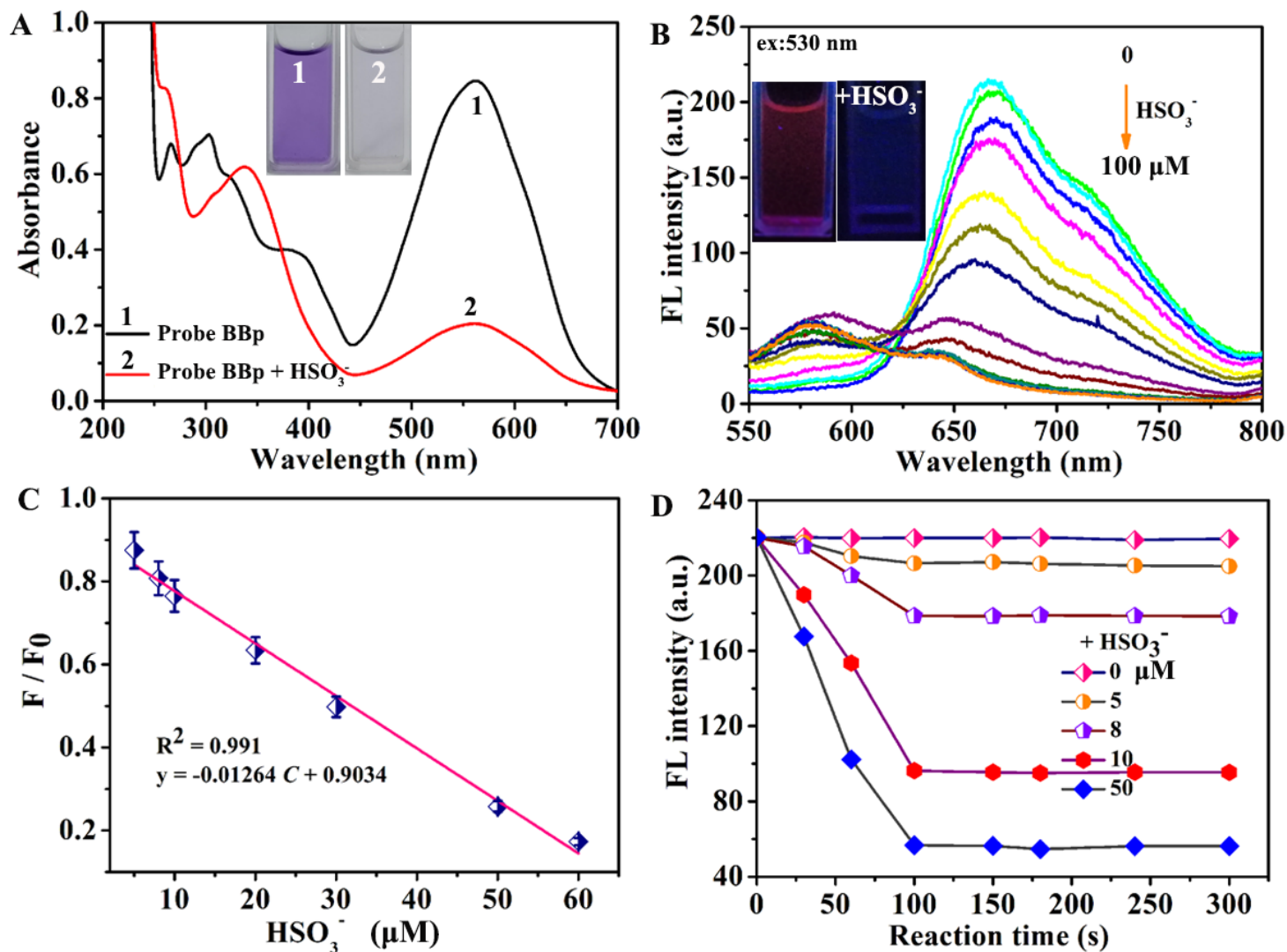


Figure 1

(A) The UV absorption spectra of probe BBp and its reaction with HSO_3^- ; (B) fluorescence spectra of probe BBp reaction with different HSO_3^- concentrations (0, 2, 5, 8, 10, 20, 30, 40, 50, 60, 70, 80, and 100 μM); (C) The linearly fitted plot of emission intensity ratio (F/F_0) of probe BBp with a certain range of HSO_3^- concentration (5, 8, 10, 20, 30, 40, 50, and 60 μM). (D) The time-dependent fluorescence intensity changes of probe BBp reaction with different concentrations of HSO_3^- (0, 5, 8, 10, and 50 μM).

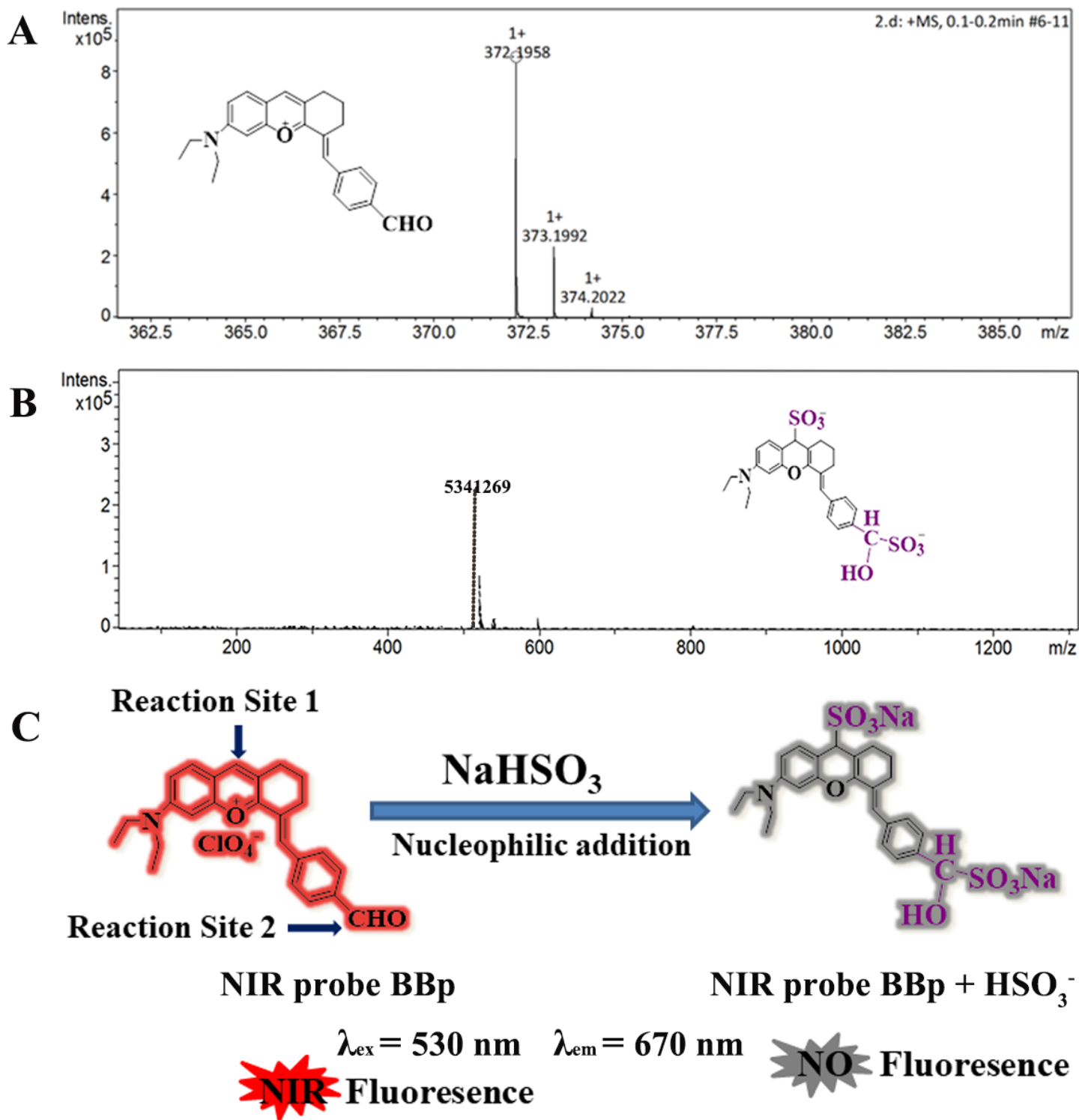


Figure 2

The HRMS spectrum of (A) probe BBp and (B) reaction with HSO₃-products. (C) The proposed sensing mechanism.

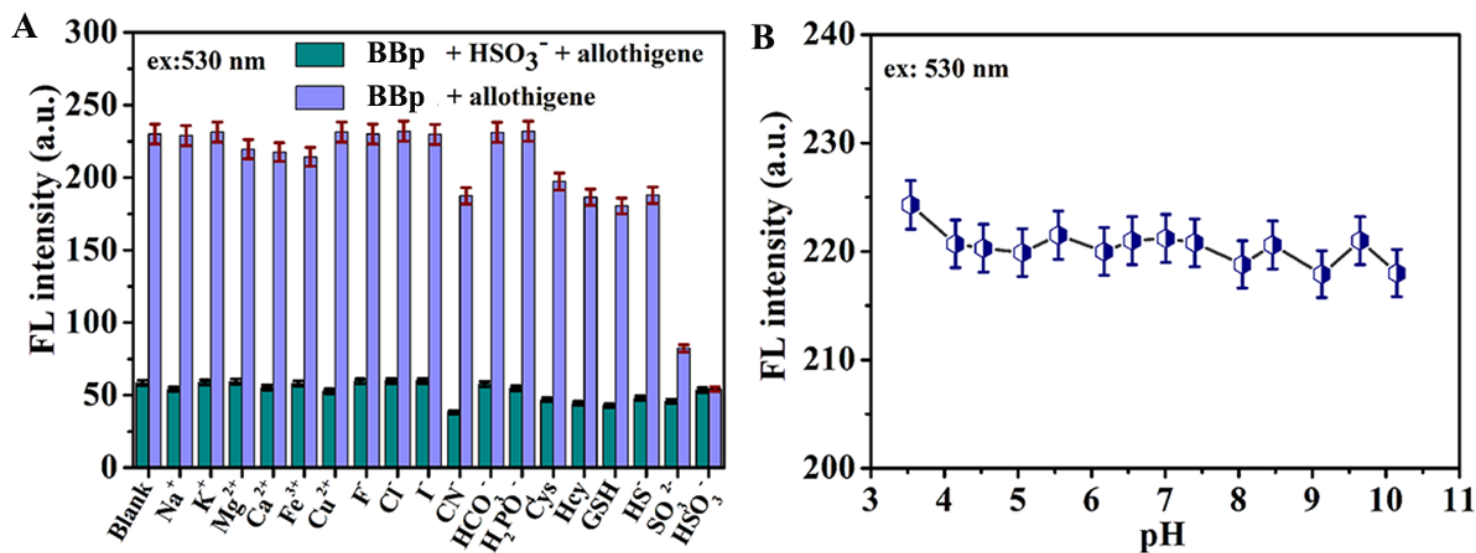


Figure 3

(A) The fluorescence intensity of BBpin the presence of allothigene. (B) Fluorescence intensity of probe BBp at different pH (3.5 – 10.5).

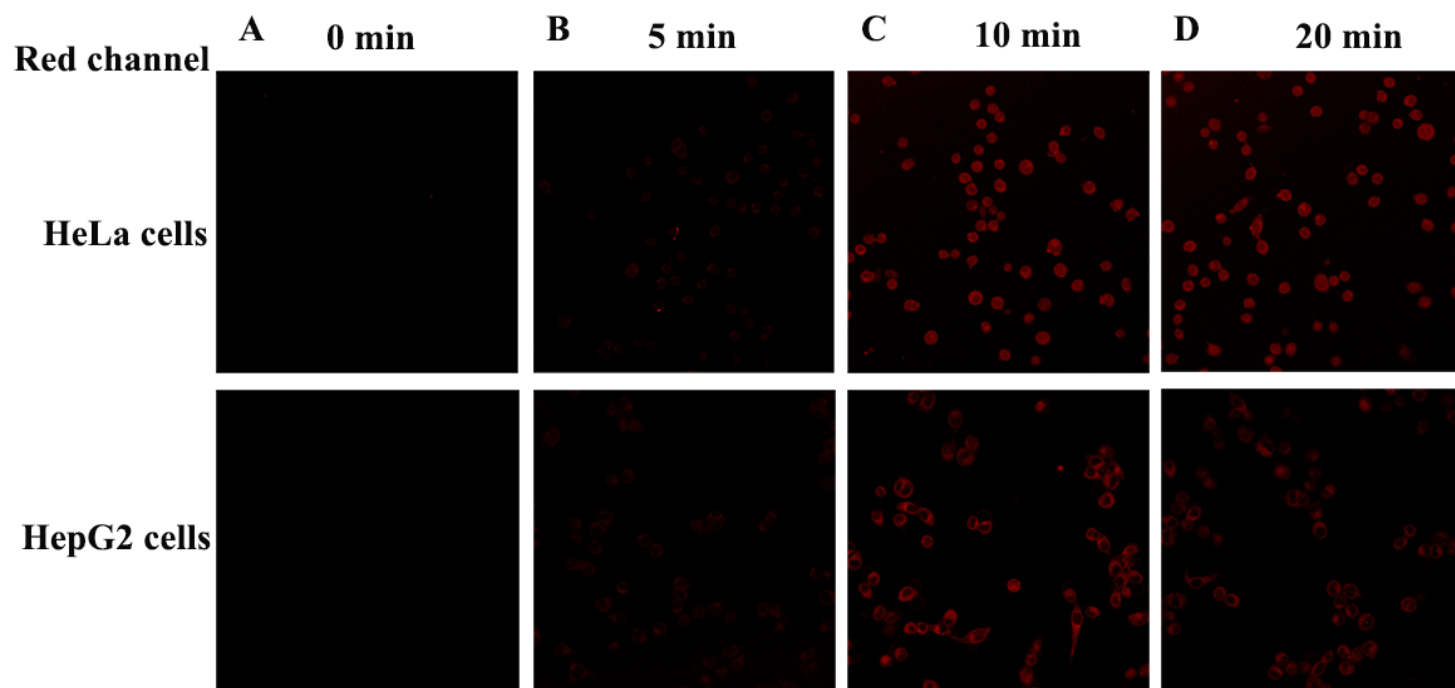


Figure 4

Fluorescent imaging of the stability of probe BBp(10 μM) incubated with HeLa cells and HepG2 at different times. Incubate at different times: (A) 0 min, (B) 5 min, (C)10 min, and (D) 20 min. The red channel: $\lambda_{em} = 566 - 697 \text{ nm}$ ($\lambda_{ex} = 561 \text{ nm}$). Scale bar = 20 μm.

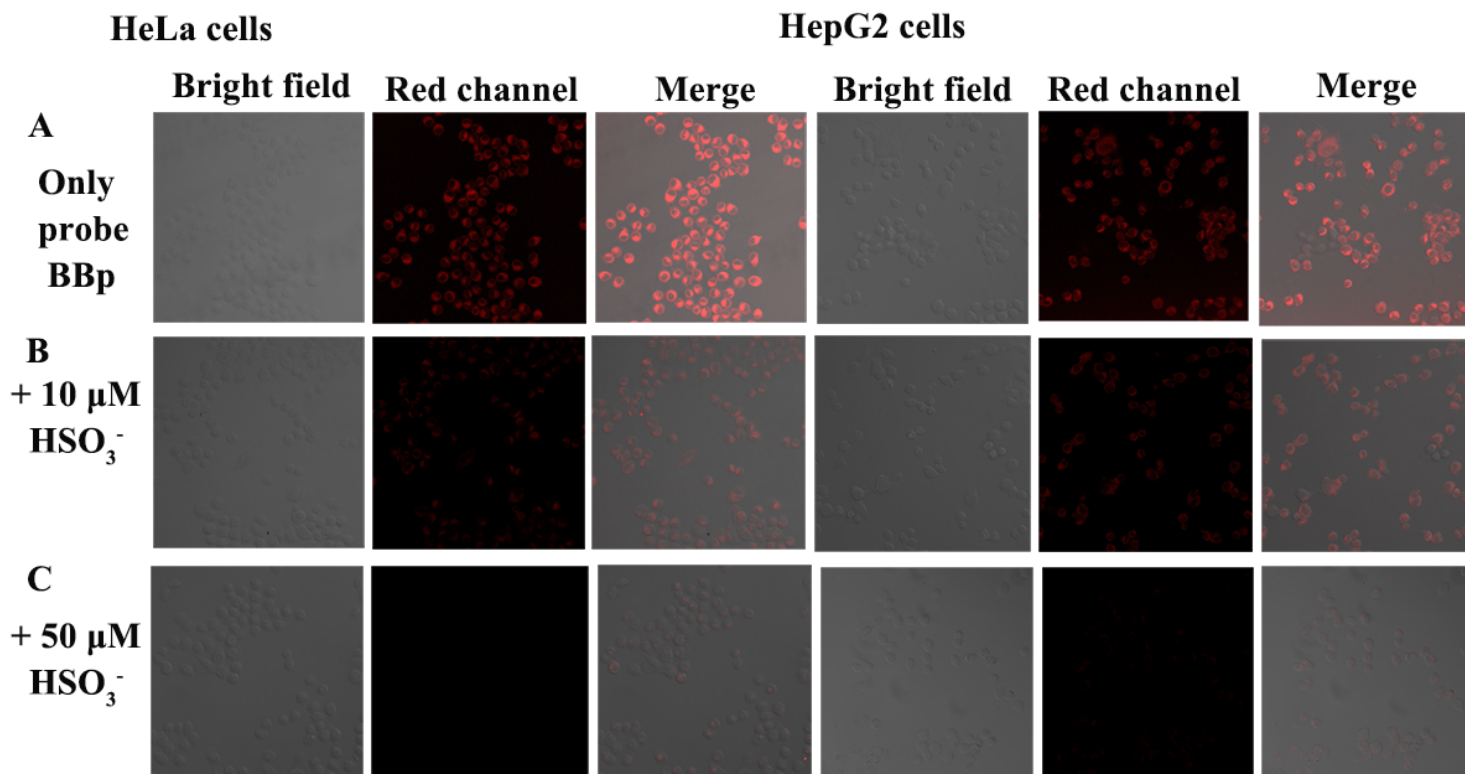


Figure 5

Fluorescent imaging of the HeLa and HepG2 cells incubated with probe BBp (10 μM) for 10 min and then treated cells with different concentrations of HSO_3^- . The concentrations of HSO_3^- (A) 0 μM , (B) 10 μM , and (D) 50 μM . The red channel: $\lambda_{\text{em}} = 566 - 697 \text{ nm}$ ($\lambda_{\text{ex}} = 561 \text{ nm}$). Scale bar = 20 μm .

Supplementary Files

This is a list of supplementary files associated with this preprint. Click to download.

- [SupplementaryMaterialYZYang.docx](#)
- [floatimage1.png](#)